Urban Forestry & Urban Greening 48 (2020) 126582

Contents lists available at ScienceDirect

Urban Forestry & Urban Greening

journal homepage: www.elsevier.com/locate/ufug

Original article

Hydrological and thermal regime of a thin green roof system evaluated by physically-based model

Vojtech Skala[a], Michal Dohnal[a,*], Jana Votrubova[a], Tomas Vogel[a], Jaromir Dusek[a], Jan Sacha[a], Vladimira Jelinkova[b]

[a] Faculty of Civil Engineering, Czech Technical University in Prague, Prague, Czech Republic
[b] University Centre for Energy Efficient Buildings, Czech Technical University in Prague, Bustehrad, Czech Republic

ARTICLE INFO

Handling Editor: Nicholas Williams

Keywords:
Design of green infrastructure systems
Extensive green roof
Heat transport
Soil water regime
Water balance

ABSTRACT

Green roofs, as an element of the green infrastructure, contribute to the urban heat island effect mitigation and the urban drainage outflow reduction. To achieve the desired functions, it is essential to understand the role of the individual roof layers and ensure their proper design.

A physically-based model was used to assess the hydrological and thermal regime of two experimental green roof test beds containing distinct soil substrates (a local Technosol and a more permeable commercial substrate "Optigreen"). The test beds together with a meteorological station were built on the building green roof. Each test bed has an effective area of one square meter and is equipped with a soil temperature sensor and an outflow gauge; one of the test beds is continuously weighed. The observed conditions were simulated using one-dimensional numerical model describing the water flow in variably saturated porous medium by Richards' equation and the heat transport by the advection-conduction equation.

The model was able to satisfactorily reproduce the measured outflow and soil temperature. The water-potential-gradient based root water uptake module effectively captured the water storage depletion between the rainfall events. The difference between the two soil substrates tested is demonstrated by the contrasting ability of the soil layers to retain water. Model representation of the thermal conditions within the green roof soils was achieved using independently evaluated thermal properties of the soils and drainage board. The model was also used to analyze the effects of the substrate depth and type of vegetation cover on the transpiration and soil water regime of the green roofs. Increasing the substrate depth causes a rise of root water uptake and induces a significant reduction of the maximal temperature. The thinner soil profiles are more sensitive to the plant species selection.

1. Introduction

Anthropogenic soil-plant systems, including green roofs, comprise an important part of the green infrastructure in urban areas and become increasingly used for their various environmental benefits. The ability of green roofs to mitigate outflow, delay outflow culmination, and change biochemical properties of passing water is frequently evaluated in scientific studies (e.g., Mentens et al., 2006; Dvorak and Volder, 2010; Li and Babcock, 2014). Analyses of green roof hydrological performance were conducted for a variety of climate conditions (Jim and Peng Lilliana, 2012; Liu et al., 2012; D'Orazio et al., 2012) and roof constructions (Rosatto et al., 2013; Guo et al., 2014).

An effective way to study hydrological functioning of green roofs is the use of mathematical models (Li et al., 2019a). In the case of simulation studies, physically-based models employing Richards' equation have recently prevailed (e.g., Hilten et al., 2008; Palla et al., 2012; Hakimdavar et al., 2014). They are often used to simulate outflow from individual rainfall episodes, e.g., design storms. Far less frequent is the use of physically-based models to study not only the roof system outflow but also its water regime, including root water uptake over a longer period (Skerget et al., 2018). Continuous evaluation of green roof soil-water regime allows a better understanding of soil-plant interactions but at the same time is considerably more demanding of data (e.g., complete micrometeorological data for determination of potential evapotranspiration).

The simulation studies also vary in the level of the green roof system schematization. From studies assessing vertical water fluxes in a single soil substrate or drainage layer (Feitosa and Wilkinson, 2016;

* Corresponding author at: Faculty of Civil Engineering, Czech Technical University in Prague, Thakurova 7, Prague 6, 166 29, Czech Republic.
E-mail address: michal.dohnal@cvut.cz (M. Dohnal).

https://doi.org/10.1016/j.ufug.2020.126582
Received 12 July 2019; Received in revised form 17 December 2019; Accepted 2 January 2020
Available online 03 January 2020
1618-8667/

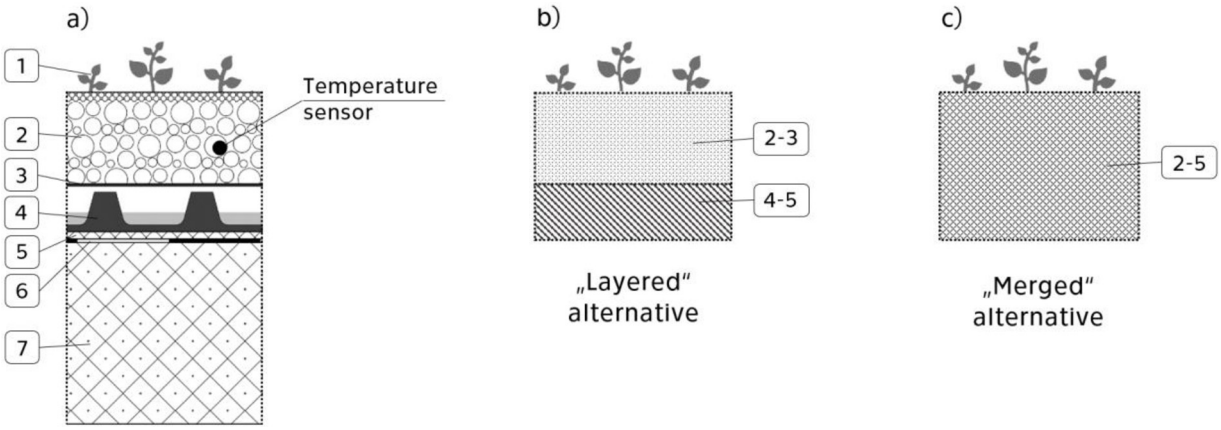

Fig. 1. a) Vertical profile of the test beds: 1. vegetation cover, 2. soil substrate 50 mm, 3. filter layer, 4. drainage layer 25 mm, 5. protection layer, 6. water-resistive layer, 7. thermal insulation 100 mm. Model representations of the green roof system: b) Layered profile and c) Merged profile.

Vesuviano and Stovin, 2013) to more complex two-dimensional simulation studies including interactions between soil and other components of the roof structure (Palla et al., 2012).

Another important aspect of green roofing – the thermal load reduction of building construction – can be evaluated by several different modeling approaches (e.g., Sailor, 2008; Tabares-Velasco and Srebric, 2012; Djedjig et al., 2012). Most frequent are physically-based models describing the heat and mass transfer through the air, plant canopy, soil medium, and building roof construction (Alexandri and Jones, 2007; Sailor, 2008). However, the vast majority of these studies do not consider water flow effects on heat transport.

As the thickness of the extensive green roofs is usually small (about 50–200 mm), the effect of atmospheric forcing on soil water and thermal regimes is crucial. Repetitive rapid changes of the green roof soil moisture status between complete saturation and dry soil are common (Savi et al., 2013). Thus, plant species with tolerance to drought and ability to withstand prolonged periods of limited transpiration are preferred (Monterusso et al., 2005; Wolf and Lundholm, 2008). At the same time, models allowing the analysis of both these extremes are needed.

The green infrastructure facilities of the University Centre for Energy Efficient Buildings (CTU in Prague) serve as a basis for studying heat load and stormwater reduction in lightweight green-roof systems. Jelinkova et al. (2015) designed simple and durable test beds equipped for automatic continuous monitoring, suitable for long-term testing of different green-roof systems. Jelinkova et al. (2016) studied the thermal and water regime of two green roof assemblies with different soil mixtures during the first months of their life cycle. The temporal changes of soil structure and composition were studied using X-ray computed tomography. Recently, two simple deterministic lumped models – a nonlinear reservoir model and a linear reservoir cascade model – were used to assess the rainfall-runoff response of the two green roof systems (Skala et al., 2019).

The objectives of the present study are twofold: (i) To reproduce the hydrological and thermal performance of extensive green roof systems with a one-dimensional numerical model of water flow and heat transport. In this respect, the soil water regime and outflow prediction for two green roof test beds are studied while two different model representations of the system (Layered and Merged) are examined. (ii) To use the numerical model as an analytical design tool. In this regard, the effects of soil depth variation and vegetation layer alteration are examined.

2. Materials and methods

2.1. Study site

The study site is on the green roof of the University Centre for Energy Efficient Buildings (UCEEB), Kladno, Czech Republic (50°09'24.8"N 14°10'10.8"E, elevation 365 m a.s.l.). The mean annual precipitation is 504 mm and the mean annual air temperature is 8.2 °C (weather station Prague – Ruzyne, 1981–2010). The corresponding values for the studied period (from April to September) are 349 mm and 14.3 °C. The present study relates to the vegetation period 2015, which was considerably drier and warmer than average – with a precipitation of only 186 mm and mean temperature of 16.5 °C (weather station UCEEB – Roof).

The building green roof (941 m^2) is located 10 m above the ground and is equipped with a complete weather station (air and substrate temperature, relative air humidity, incoming and outgoing shortwave and longwave radiation, wind speed, wind direction, and precipitation). The data are recorded with one-minute resolution. Aggregated five-minute series were compiled to be used in our numerical experiments.

2.2. Green roof test bed assemblies

In 2014, two raised green roof test beds were established on the UCEEB building green roof nearby the weather station (at a distance of about 5 m). The test beds were fully operational in 2015. Each test bed has an area of 1 m^2, a total depth of 175 mm (Fig. 1), and a slope adjusted to 2 % (for detail see Jelinkova et al., 2015, 2016). The beds contain 50 mm of distinct soil substrates. One was filled with stripped local topsoil with admixed crushed expanded clay and bricks having a dry bulk density of 1.15 kg m^{-3} (hereafter labeled TECH), the other with commercial green roof substrate Optigreen Type E (Optigrün International AG) having a dry bulk density of 0.77 kg m^{-3} (hereafter labeled OPTI). The standard commercial drainage and storage board OPTIGREEN FKD 25 (Optigrün International AG) was used in both test beds. In TECH bed, the board was installed with large naps facing up having the water retention capacity of approx. 5.0 mm, while in OPTI bed, it was installed with small naps facing up having the retention capacity of approx. 3.6 mm. Both test beds were planted with a mixture of stonecrops (*Sedum album L., Sedum hybridum L., Sedum spurium M. Bieb., Sedum acre L.*). The complete vertical profile of the studied green roof test beds is shown in Fig. 1a.

Each test bed was equipped for continuous monitoring of the soil substrate temperature (109 Temperature probe, Campbell Sci. Ltd.; at the depth of 35 mm) and the drainage layer outflow (purpose-built tipping bucket flowmeter). The OPTI test bed is weighed (load cells LCMAD-50, Omega Eng. Inc.). Five-minute weight averages calculated

based on 10-second measurements are recorded.

2.3. Soil water flow and heat transport model

One-dimensional vertical flow of soil water is described by Richards' equation:

$$\frac{\partial \theta}{\partial t} = \frac{\partial}{\partial z}(K(\frac{\partial h}{\partial z} + 1)) \quad - S \tag{1}$$

where θ is the volumetric soil water content ($m^3\,m^{-3}$), h is the soil water pressure head (m), K is the soil hydraulic conductivity ($m\,s^{-1}$), S is the intensity of root water uptake (s^{-1}), t is time (s), and z is the vertical coordinate (m) assumed positive upwards. The governing equation is solved numerically by the computer code S1D (Vogel et al., 2010a, 2010b).

A substantial component of the green-roof system water balance is the plant transpiration, implemented in the model via the root water uptake. Therefore, evaluation of the root water uptake term S is a crucial part of the simulation. In this study, the water-potential-gradient formulation of the root water uptake (WPG approach), as implemented in the S1D code (Vogel et al., 2013, 2016), was used. This approach considers the root water uptake to be distributed according to the water availability and allows roots to redistribute the soil water between wet and dry layers.

The WPG approach assumes that the water flux between the soil and the plant roots is forced by the difference of water potential between the soil and the root xylem. At the same time, it is controlled by the hydraulic resistances along the way:

$$S(z) = \frac{2\pi r_0 R(z)}{r_{soil}(z) + r_{root}}[H_{soil}(z) - H_{rx}] \tag{2}$$

where r_0 is the average active root radius (m), $R(z)$ is the root length density (m^{-2}), r_{soil} is the soil hydraulic resistance (s), r_{root} is the root radial resistance (s), H_{soil} is the bulk-soil water potential (m), and H_{rx} is the root xylem water potential (m). The soil resistance r_{soil} is evaluated based on the soil hydraulic conductivity and the characteristic length associated with water transport from the bulk soil to the root surface (Vogel et al., 2016).

An integral of S over the depth of rooting defines the plant transpiration rate, E_T ($m\,s^{-1}$):

$$E_T = \int_{z_R}^{z_0} S(z)dz \tag{3}$$

where z_0 and z_R represent the coordinates of the upper and lower boundary of the root zone (m), respectively.

At each time step of the numerical solution, the root xylem water potential, H_{rx}, is evaluated so that the calculated transpiration rate meets the prescribed potential transpiration, $E_T = E_{Tp}$. If H_{rx} for a given potential transpiration rate falls below a critical value of H_{crit}, H_{rx} is set equal to $H_{crit,}$ and a reduced actual transpiration rate, $E_{Ta} < E_{Tp}$, is calculated. The H_{rx} value is then used to calculate the root water uptake intensity $S(z)$ (from eq. 2) and to update the value of the sink term in eq. 1.

The heat transport is described by the advection-conduction equation implemented into S1D code (Vogel et al., 2011):

$$\frac{\partial CT}{\partial t} + \frac{\partial qC_w T}{\partial z} - \frac{\partial}{\partial z}(\lambda\frac{\partial T}{\partial z}) = -SC_w T \tag{4}$$

where C is the volumetric heat capacity ($J\,m^{-3}\,K^{-1}$), T is the soil temperature (K), q is the soil water flux ($m\,s^{-1}$), C_w is the volumetric heat capacity of water ($J\,m^{-3}\,K^{-1}$), and λ is the soil thermal conductivity ($W\,m^{-1}\,K^{-1}$).

To express the soil thermal conductivity as a function of the soil water content, the methodology proposed by Côté and Konrad (2005) is used.

2.4. Model application

2.4.1. Simulation period and model discretization

The S1D model is used to simulate water and heat fluxes in the green roof test beds during the vegetation period 2015 (April 1st through September 30th). The test beds are approximated by a vertical one-dimensional 75-mm-deep soil column. Two levels of schematization are tested for the water flow and heat transport simulations: (1) in the Layered alternative, the substrate and the drainage board layers are described separately by distinct sets of hydraulic and heat transport parameters based on individual properties of each material (Fig. 1b); (2) in the Merged alternative, the whole system is assumed homogeneous, represented by a single set of effective hydraulic and heat transport parameters (Fig. 1c).

2.4.2. Boundary conditions

For water flow model, the measured precipitation intensities, aggregated in 5 min time steps, are used to define the flux at the upper boundary. Surface runoff is not considered because it was not observed. At the bottom, a seepage face boundary condition is imposed allowing water to leave the test bed under saturated conditions. The potential evapotranspiration of the stonecrops is estimated hourly using the Penman-Monteith equation (Monteith, 1981), and is used to evaluate the root water uptake. For the heat transport model, a variable surface temperature prescribes the upper boundary. The temperature is determined from the measured outgoing long-wave radiation using Stefan-Boltzmann law assuming that the ground behaves like a perfect blackbody. The radiation is measured directly at the roof over the roof surface with the same composition as the TECH test bed. As the test beds are heavily insulated at the sides and bottom, zero gradient condition is assumed at the bottom boundary. Still, the heat can leave the system at the bottom by advection.

2.4.3. Hydraulic parameters

Initially, the hydraulic parameters of separate layers were evaluated independently. For the soil substrates (Jelinkova et al., 2015), the retention curve was determined combining information obtained from the particle size distribution and bulk density using the neural network model Rosetta of Schaap et al. (2001) with the results of standard laboratory methods (sand bed and pressure plate apparatus) applied to 100 cm^3 packed samples. The saturated hydraulic conductivity K_s was estimated based on a laboratory ponded infiltration experiment performed on large packed samples (1,000 cm^3). The drainage board parameters were set to mimic the board characteristics provided by the manufacturer (Table 1). As the board can be completely dry, the residual water content θ_r is set to zero. The values of saturated water content θ_s and the retention curve shape parameters α_{VG} and n_{VG} were set to ensure that the retention capacity of the drainage board (reported by the manufacturer) was reproduced (maximum retention capacity of the TECH bed is 7.4 mm in the soil profile and 5 mm in the drainage board; for the OPTI bed, it is 0.8 mm and 3.6 mm, respectively). The saturated hydraulic conductivity was set to 5,000 cm d^{-1} to allow fast drainage. The resulting parameters of the drainage board are similar to those of a coarse material (e.g., gravel).

To achieve optimal model performance, hydraulic parameters of the soil substrates were upscaled by means of parameter optimization procedure. PEST software package for model-independent parameter estimation (Doherty et al., 1994) based on the Levenberg-Marquardt algorithm for nonlinear optimization (Marquardt, 1963) was used. The sum of squared residuals between the measured and simulated cumulative outflow served as an objective function. Specifically, the water retention parameters α_{VG}, n_{VG}, and θ_s, as well as the saturated hydraulic conductivity, were optimized. The resulting parameter values are shown in Table 1. Relative changes in values of saturated water content before and after upscaling procedure were about 30 %. The hydraulic conductivity and soil water retention parameter n_{VG} exhibited changes

Table 1
Hydraulic parameters of the test beds.

Alternative	Layer	Depth (mm)	θ_r ($cm^3\,cm^{-3}$)	θ_s ($cm^3\,cm^{-3}$)	α_{VG} (cm^{-1})	n_{VG} (–)	K_s ($cm\,d^{-1}$)
TECH – Layered	soil	50	0.05	0.380	0.54	1.77	64.7
	drainage board	25	0.00	0.235	0.45	2.70	5,000
TECH – Merged	merged profile	75	0.05	0.328	0.30	2.66	78.6
OPTI – Layered	soil	50	0.05	0.254	0.76	3.08	687
	drainage board	25	0.00	0.169	0.45	2.70	5,000
OPTI – Merged	merged profile	75	0.05	0.250	0.68	3.05	872

θ_r and θ_s are the residual and saturated water contents, K_s is the saturated hydraulic conductivity, and α_{VG} and n_{VG} are shape parameters (van Genuchten, 1980).

up to 170 %. Changes in the order of magnitude occurred in the empirical parameter α_{VG}. Residual water contents and the drainage board parameters were fixed at their original values.

2.4.4. Root water uptake parameters

For the root water uptake model, the root length density of stonecrops within the test bed is assumed depth-invariant with a value of R = 0.3 cm^{-2} (the value is within the generally reported range for field-grown plants, Perez-Harguindeguy et al., 2013). The average active root radius is set equal to a constant value of r_0 = 0.014 cm (similar value was reported by Ji et al. (2018) for *Sedum album*), and the threshold value of the root xylem water potential H_{crit} = –150 m (e.g., Bechmann et al., 2014). The radial hydraulic resistance of the root tissues was determined by sequential optimization. The upscaling procedure of hydraulic parameters was repeated for four values of root resistances: 1,000, 7,500, 10,000, and 15,000 d. The optimal value of the root resistance was found to be r_{root} = 7,500 d.

2.4.5. Heat transport parameters

Thermal properties are assessed using methodology of Côte and Konrad (2005) (Table 2). Heat capacities and thermal conductivities of all constituents (i.e., water, organic matter, plastic drainage board, air, granite contained in TECH and mixture of expanded shale, pumice, bricks and compost contained in OPTI) were set to the values from the literature (e.g., Hillel, 1998; Kodešová et al., 2013). The bulk heat capacities and thermal conductivities given in Table 2 are calculated based on these values and volumetric fractions of each constituent. Note that for the drainage boards, most of the volume is permanently occupied by air and the organic matter fraction accounts for roots reaching into the drainage board. The thermal properties of the dry soil substrates (volumetric heat capacities and thermal conductivities) were also measured both in the laboratory and *in-situ* using ISOMET 2114 (Applied Precision Ltd.). Resulting values were in a good agreement. The soil thermal dispersivity is set equal to 0.5 cm. Assuming nearly linear relationships between bulk soil thermal conductivity and the soil water content, soil-type factor κ is 0.95 for the soil substrates. For the drainage boards, κ is set 0.6 to allow a faster decrease of conductivity when the board is drained.

2.4.6. Performance criteria used

The ability of the model to predict the water and thermal regimes is evaluated by the Nash–Sutcliffe model efficiency NSE (Nash and Sutcliffe, 1970) and root mean square error RMSE.

2.4.7. Design simulations

The S1D model was used to test how the green roof changes affect its hydrological and thermal regime. Specifically, the effect of the soil substrate depth and the vegetation type was examined. The substrate depth was varied between 25 and 150 mm. Sedum plants can survive with only 25 mm of the substrate (van Woert et al., 2005) and 150 mm is often stated as the upper boundary for extensive green roofs. Changing vegetation was imitated by varying the root resistance r_{root} from 1,000 to 15,000 d, covering a wide spectrum of plant types (from maize and soybean to woody plants as reported by Rieger and Litvin (1999) or tomato and other agricultural plants mentioned in Zwieniecki and Boersma (1997) and de Jong van Lier et al. (2013)).

Another effect of the added substrate – the increasing weight of the green roof – was examined (again in the range of substrate depths 25–150 mm). The total weight of the green roof includes: (1) layer with changing weight (substrate of selected depth and maximal water content that occurred during simulation of vegetation season), and (2) layers with constant weight (filter textile layer 0.4 kg m^{-2}, drainage board considered as full of water – 6.4 kg m^{-2} in case of TECH and 5.0 kg m^{-2} in case of OPTI, protection textile layer 0.4 kg m^{-2}, and water-resistive layer 1.3 kg m^{-2}).

3. Results and discussion

3.1. Water balance components

Table 3 shows the water balance components for both test beds evaluated for the studied period (from April 1st to September 30th, 2015). Nearly twofold outflow height was observed for the OPTI bed compared to the TECH bed reflecting the difference in water retention capacity between the two systems; both the soil substrate and the drainage board of the TECH test bed provide larger water retention capacity than their counterparts in the OPTI test bed (Table 3).

The model results slightly underestimate the outflow in all cases (in TECH bed by about 3 %, in OPTI by about 4 %). For both test beds, the Layered alternative provides more accurate outflow predictions. It should be noted that the overall good agreement between the model and observation comes from the model having been optimized to

Table 2
Thermal properties of the test beds.

Alternative	Layer	Depth (mm)	λ_{dry} ($W\,m^{-1}\,K^{-1}$)	λ_{sat} ($W\,m^{-1}\,K^{-1}$)	κ (–)	C_s ($kJ\,kg^{-1}\,K^{-1}$)	ε_s (–)	ε_o (–)
TECH – Layered	soil	50	0.158	0.706	0.95	1.913	0.420	0.200
	drainage board	25	0.037	0.077	0.60	2.300	0.060	0.100
OPTI – Layered	soil	50	0.226	0.565	0.95	1.368	0.639	0.107
	drainage board	25	0.037	0.063	0.60	2.300	0.060	0.100

λ_{dry} and λ_{sat} are the soil thermal conductivities for dry and saturated soil, respectively, κ is a shape parameter dependent on the soil texture and composition (Côte and Konrad, 2005), C_s is the heat capacity of solids, ε_s, ε_o are soil constituent – mineral and organic – fractions.

Table 3
Water balance components of the green roof test beds for the studied period. Measured rainfall, observed outflow, prescribed potential transpiration, as well as simulated outflow and actual transpiration are presented for two simulation alternatives for each of the two test beds.

Alternative	Rainfall (mm)	Observed outflow (mm)	Simulated outflow (mm)	E_{Tp} (mm)	E_{Ta} (mm)
TECH – Layered	186.0	44.6	43.6	556.5	142.4
TECH – Merged	186.0	44.6	42.8	556.5	143.2
OPTI – Layered	186.0	80.2	76.8	556.5	109.2
OPTI – Merged	186.0	80.2	75.8	556.5	110.2

provide good cumulative outflow prediction (presented in right-hand side panels of Fig. 2).

The 33-mm difference in the simulated outflow between the beds is mirrored by the difference in the actual transpiration. This again reflects the ability of the TECH bed components to hold more water, which can subsequently be used for plants transpiration. However, the reduction of transpiration is significant for both test beds, i.e., the actual transpiration comprises only 26 % and 20 % of the potential transpiration for TECH and OPTI test bed, respectively.

3.2. Rainfall-runoff relationship

The performance of the soil water flow model is demonstrated by comparing simulated and observed outflows (Fig. 2). The response of the two test beds to a major rainfall event is shown in the left-hand side panels. The event started on August 16th, and the total rainfall was 49.8 mm. The outflow during the event is satisfactorily simulated for the OPTI test bed (NSE higher than 0.7). For the TECH bed, the simulated outflow is considerably delayed as compared to the observations, which is reflected by the NSE criterion about 0.23. Still, the total outflow volume during this outflow event is matched very well.

Note that our results, obtained for test beds with an area of 1 m^2, are representative for real green roofs regarding the retention function (i.e., reduction of the runoff volume) and have only limited relevance regarding the detention function (i.e., delay and redistribution of the runoff over time), which would become dominated by lateral flow effects as the roof area increases (e.g., Palla et al., 2011).

Vesuviano and Stovin (2013) studied in detail hydrological response of a drainage board. They concluded that simple storage routing models or power-law relationships are capable of mimicking hydrological functioning of the drainage layer. Skala et al. (2019) came to similar conclusions for a complete green roof system. However, they found episodically applied models, considering the same initial retention

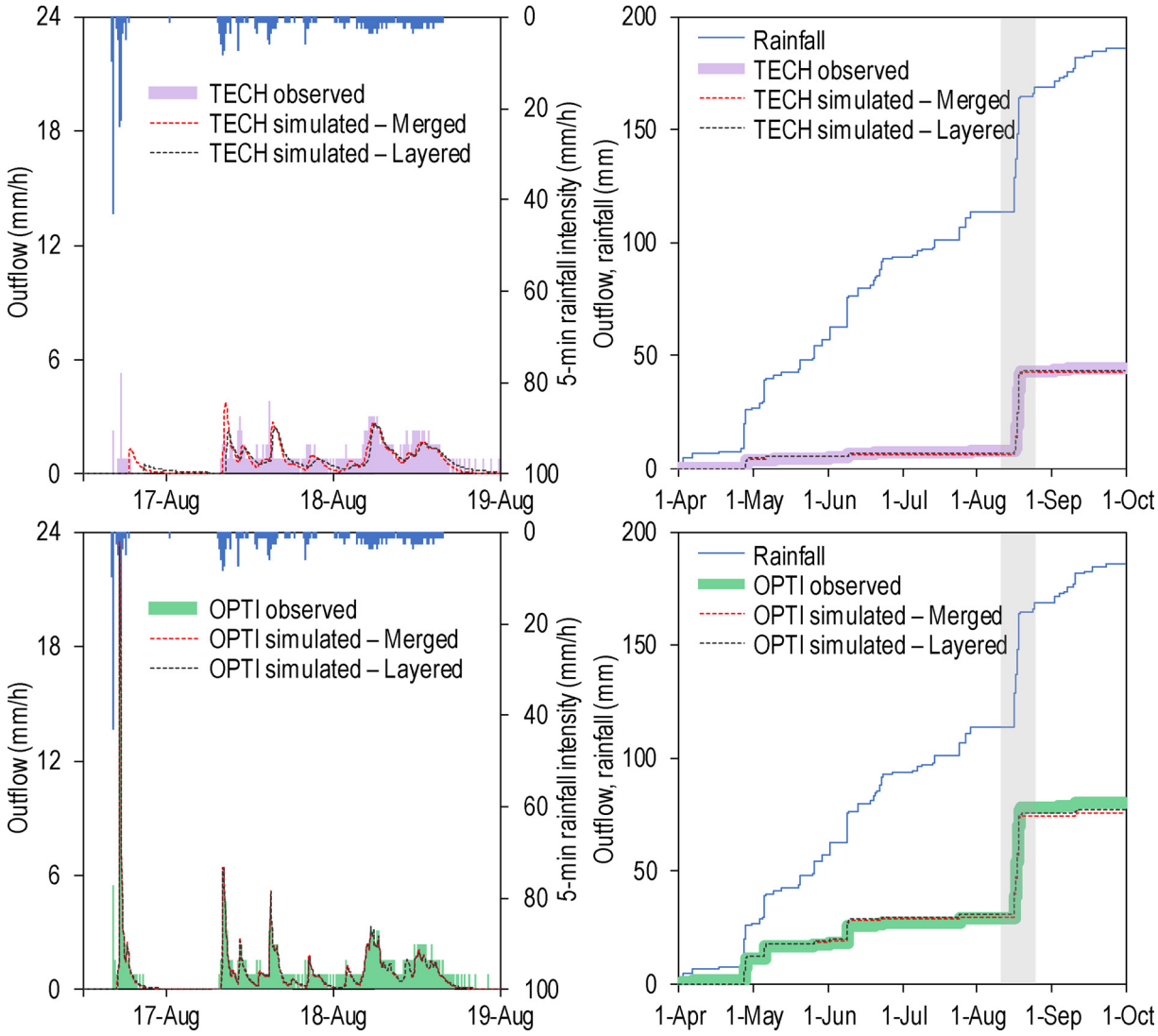

Fig. 2. Comparison of observed and simulated test bed discharges during the August rainfall-runoff event (left) and the whole vegetation season 2015 with the August event marked in gray (right).

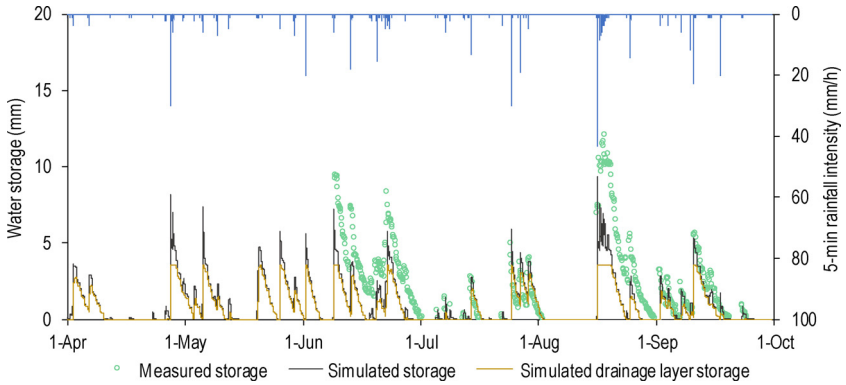

Fig. 3. Measured and simulated water storages in OPTI test bed (Layered alternative).

storage for all episodes, insufficient for green-roof segment with a high retention capacity. Simulation models accounting for evapotranspiration and the respective soil water status development between the rainfall events are needed. Nonlinear reservoir model of Skala et al. (2019) applied to the same green roof data exhibited average NSE = –0.5, while in the present study, with the use of physically-based model allowing for realistic root water uptake, NSE was about 0.2.

The drainage layer together with the bottom boundary condition play an important role in hydrological modeling of green roof systems. The two-layer model with an explicit drainage layer can be substituted by a single-layer model with uniform effective hydraulic properties, which however, must reflect the retention properties of the whole system including drainage board, not only of the soil layer. In our study, the hydraulic parameters of the Merged model are determined by means of inverse modeling and provide similar results as the Layered alternative (see Table 3 and Fig. 2).

3.3. Water retention and root water uptake

Temporal changes of the water amount stored in the OPTI test bed are presented in Fig. 3. The observed water storage was determined from the test bed weight by subtracting the dry weight of the assembly (76.5 kg). The simulated water storage was computed by the Layered alternative of the model. The courses of simulated and measured water storages are very similar (R^2 = 0.873, NSE = 0.750). However, the storage during and after rainfall events with rainfall exceeding 12 mm (e.g., June and September) is strongly underestimated.

Further analysis of Fig. 3 reveals that water storage in the drainage layer is a dominant component of the total OPTI bed storage during the studied period.

The spatiotemporal distribution of the simulated root water uptake S in the two test beds (Layered alternative) is depicted in Fig. 4 (darker color indicates the greater intensity of the root water uptake). This figure illustrates the different character of root water uptake in OPTI and TECH beds. As the TECH bed retains most of the water in the substrate (in average 4 times more than in the drainage layer, time-averaged storages in soil substrate and drainage layer are 2.65 mm and 0.64 mm, respectively), water for the plants is dominantly taken from this layer. For more permeable OPTI test bed, water for the plants is mostly available from the storage capacity of the drainage board.

The maximal rate of predicted actual transpiration is the same for both test beds as it is defined by the root water uptake parameters describing the plant (r_{root}, r_0, R, H_{crit}) and is achieved only if the water is available throughout the whole rooting depth. As a certain part of the profile dries out, the root water uptake from that part becomes regulated by the increasing soil resistance and the total transpiration rate reduces.

The advantage of the approach used is that it can handle the spatial distribution of root water uptake while accounting for the availability of water throughout the rooting zone. On the other hand, there is a lack of relevant parameter values for plants used in green roofs in the literature. In addition, some of the suitable plants (selected species from the *Sedum* genus) exhibit behavior not accounted for in our model (switching between C3 photosynthesis and CAM metabolism and vice versa during single vegetation season with prolonged drought periods (Starry et al., 2014)).

3.4. Thermal regime

Generally, the measured variance of soil temperature oscillations is expected to decrease markedly with the depth of the soil substrate. In addition, the peak temperatures are delayed. In the green roof system and vegetation season studied, the daily peak temperature amplitudes were reduced in green roof system by 6 °C in maximum and at the same time temperature peak was delayed by five hours.

Thermal regime of TECH test bed (Layered alternative) is documented in Fig. 5. Simulated and observed temperatures are presented for an eight-day period including the major precipitation event. During the first three days, the reduction and delay of the peak temperature between the soil surface (used as a boundary condition) and the soil substrate is clearly visible. During the rainfall episode, all temperatures become similar; the temperature of the soil substrate is cooled to a temperature of precipitation, which is in equilibrium with air. The match between simulated and measured soil temperatures is reasonably good (applies also for Merged system simulations – not shown here), still, discrepancies are evident during the peak temperatures when the substrate is dry (before the rainfall) and during the cooling phases when the substrate is wet (after the rainfall). In this context, note that the heat transport parameters were not *ad hoc* calibrated.

An overall comparison of the measured and simulated soil temperatures at a depth of 35 mm is shown in Fig. 6. The soil temperatures in both test beds are predicted with high consistency (NSE TECH = 0.97 and NSE OPTI = 0.98). The temperature predictions for the OPTI bed are more scattered in comparison with TECH. On the other hand, in the TECH test bed, temperatures above 25 °C are systematically overestimated.

3.5. Design simulations

Note, that our design simulations are built on relatively crude assumptions. First, hydraulic parameters determined for a 50-mm deep soil layer are used while the depth of the substrate is varied. Secondly, the soil substrate depth is likely to alter the thermal regime completely, including the temperature at the soil surface. However, presented heat transport simulations are conducted with the upper boundary condition unchanged among the variant simulations. Nevertheless, we believe that the results are relevant and valid for the systems studied.

The effect of the substrate depth on the simulated cumulative

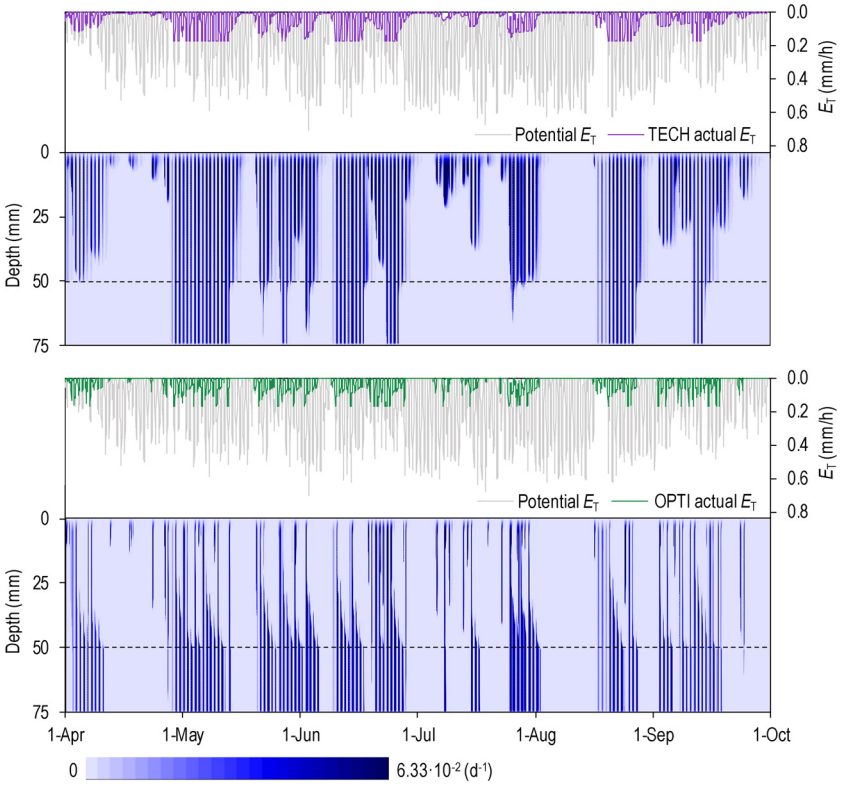

Fig. 4. Simulated spatiotemporal distribution of root water uptake for TECH and OPTI test beds (Layered alternative).

transpiration is shown in Fig. 7. Increasing the substrate depth causes a rise of root water uptake/transpiration due to increasing retention capacity and longer travel times of the substrate. The effect of increasing retention capacity is more pronounced for smaller depths of TECH (the nonlinear part of the respective curves in Fig. 7a). It is negligible for the OPTI test bed because the shape of OPTI retention curve (between 50 and 150 mm of substrate depth, the retention capacity expands by 0.2 mm only). Over the range of depths tested, the depth-increase related E_{Ta} change for OPTI is predominantly caused by the increasing time period after rain cessation available for water to pass through the substrate. Thus the increase of E_{Ta} is almost linear (Fig. 7a). This is consistent with the expectation that the hydrological response of highly-permeable substrates (with limited retention capacity and high hydraulic conductivity) is less affected by their depth. The importance of drainage layer decreases with increasing depth of the soil substrate.

Many studies omitted the drainage layer in the model structure used (e.g., Hilten et al., 2008; Yang et al., 2015; Hakimdavar et al., 2014). Together with different climatic conditions, this is probably the reason for considerably lower retention capacity of the vegetated soil layer as reported by Feitosa and Wilkinson (2016). They determined retention of soil substrate similar to TECH to be between 28 and 32 % of total rainfall (for 40 mm and 200 mm deep soil, respectively). In our study, the drainage board covered by 25 mm and 150 mm deep soil added about 27 and 2 % to the seasonal storage, respectively.

The increase of cumulative transpiration with increasing substrate depth is accompanied by the corresponding decrease of cumulative outflow (not shown here). This is in agreement with the earlier studies of Feitosa and Wilkinson (2016) or Soulis et al. (2017). Li et al. (2019b) analyzed the hydrological benefits (e.g, reduction of outflow and increase of transpiration) of green roofs with increasing storage in drainage layer. The authors suggested that there is a critical substrate depth for which the slope of the cumulative outflow curve becomes significantly less steep compared to lower substrate depths. Above the critical depth the efficiency of further increasing the substrate depth diminishes. In our case, the modeling results indicate that the critical depth is about 60 mm for both TECH and OPTI bed (Fig. 7a).

Apart from changing depth, the impact of the plant species alteration was tested. The vegetation cover change was simulated by varying the radial root resistance parameter of the root water uptake model. Different plant species have different radial root resistance reflecting their water-use strategy. Simulated actual transpiration in reaction to changing substrate depth and plant radial root resistance is presented in Fig. 7b. It is clear that thinner soil profiles are more sensitive to plant species change. In general, when designing green roofs with thin (the

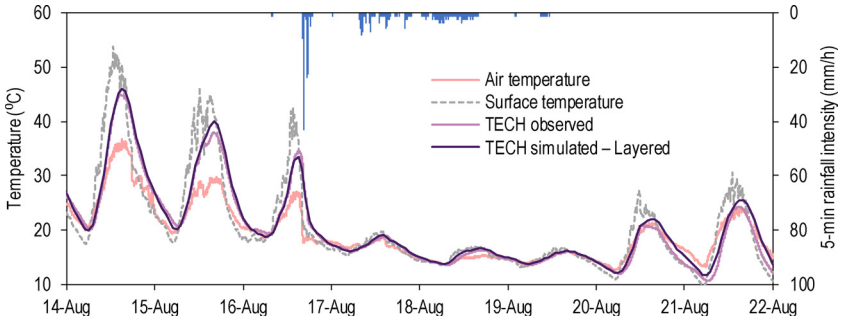

Fig. 5. Soil temperatures measured and simulated at a depth of 35 mm during the August rainfall-runoff event. Upper boundary conditions of the simulation: surface temperature determined from the measured outgoing long-wave radiation and rainfall intensity, are given together with air temperature measured nearby at 200 cm above the ground.

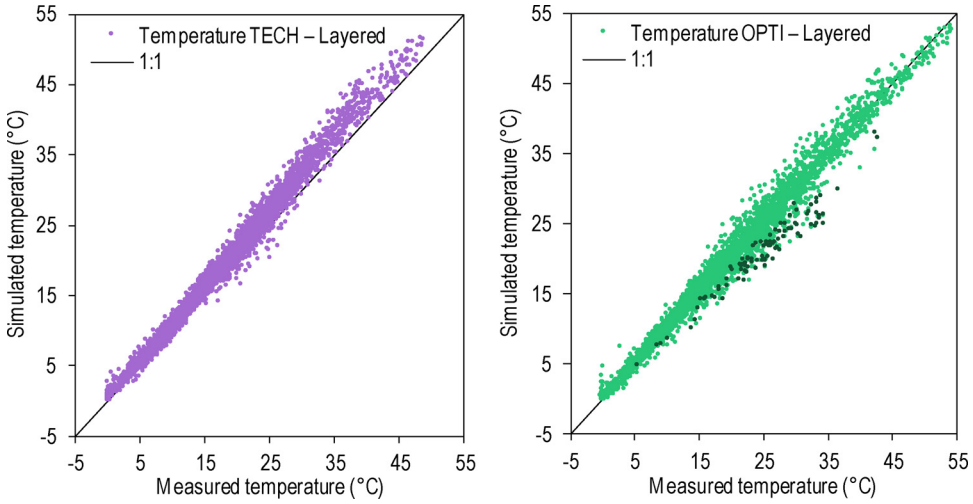

Fig. 6. Measured and simulated temperatures at a depth of 35 mm of TECH and OPTI test beds. Darker dots of OPTI bed indicate measured soil temperature at 35 mm depth that was higher than measured soil surface temperature used as an upper boundary condition. RMSE criterion of measured and calculated temperatures for TECH and OPTI test bed was 3.2 and 2.3 °C, respectively.

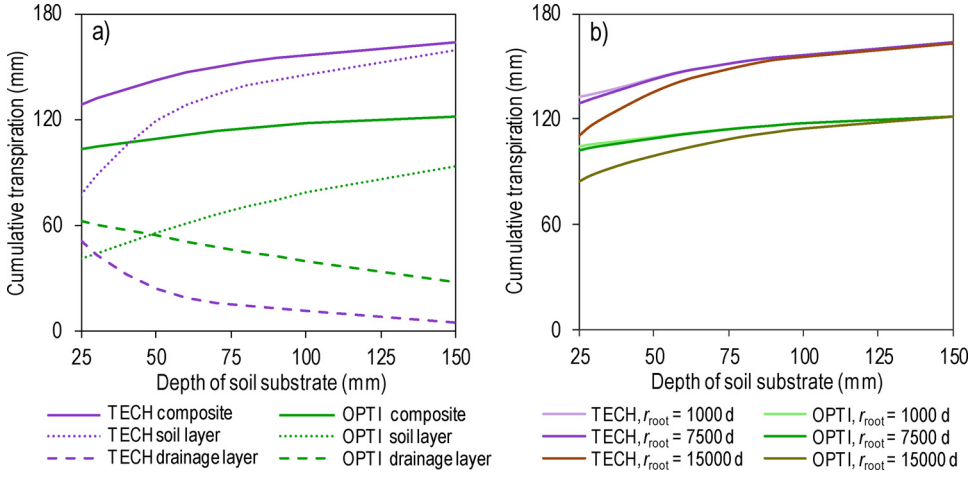

Fig. 7. Simulated cumulative transpiration as obtained for different depths of soil substrate and different vegetation type represented by a considerably different radial root resistance: a) contributions of soil and drainage layers to cumulative actual transpiration – assuming r_{root} = 7500 d, and b) the effect of different radial root resistance.

depth less than 75 mm) soil substrate layer, the plant species selection seems to be a critical aspect.

Additionally, the effect of the soil substrate thickness on the thermal condition was inspected. While the average simulated temperatures at the bottom of the soil layer remain unchanged, increasing depth of the soil substrate induces a slight growth of the minimal temperatures and a significant reduction of the maximal temperature (by about 15 °C) in both test beds (Fig. 8). This reflects the fact that adding more matter increases thermal inertia of the whole system.

Finally, it should be noted that the depth of the substrate significantly affects the total weight of the roof structure. Water storage in soil represents only a minor part of the total weight, i.e., about 16 % in the case of TECH system and about 11 % in OPTI system. Remaining layers (filter layer, drainage layer with water, protection layer, and water-resistive layer) take a similarly small part of the total weight. The major part of the load of green roofs is due to the soil substrate.

3.6. Experimental and model limitations

The fact that the model underestimates both the outflow and the water storage (e.g., Fig. 3) is partly related to the difficulties associated with the measurements of high outflow rates (affecting the model parameters via the upscaling optimization procedure). Another model limitation could be associated with the effects of bimodal porosity of the OPTI substrate. Bimodal porosity may affect the retention properties of the soil (Durner, 1994). In artificially prepared soil substrate, natural soil aggregates are substituted by expanded shale, expanded

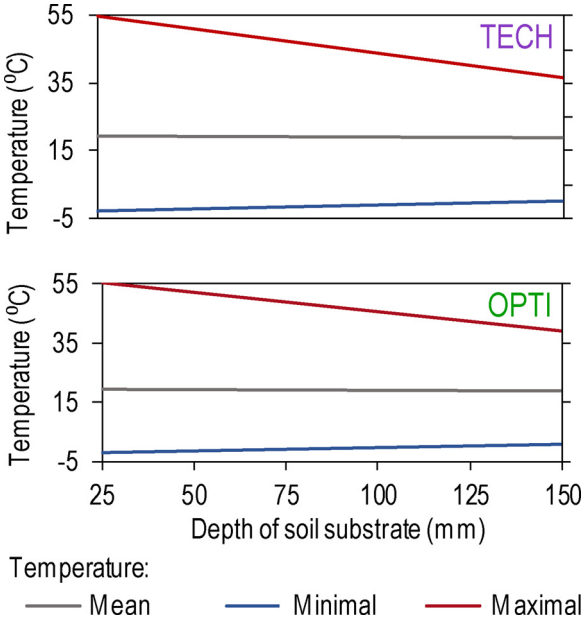

Fig. 8. Simulated temperatures (for both test beds, Layered alternative) as function of the depth of soil substrate.

clay, lava, pumice, or crushed brick. These materials have fine pores and correspondingly low hydraulic conductivity. When water infiltrates into a dry mixture, it tends to bypass these components. Thus, the pore space inside these porous particles is not immediately filled with water; it can be filled only if the wet conditions prevail for a sufficiently long time. Such behavior is not considered in our model, and thus, it is not reflected in the simulation results. The fact that the effective saturated water content of the OPTI substrate used in our simulation ($0.254\ cm^3\ cm^{-3}$) is lower than that reported by the manufacturer ($0.35\ cm^3\ cm^{-3}$) fits the hypothesis.

The presented analysis benefits from the fact that the available observation period – vegetation season 2015 – was dryer than average yet contained a number of significant rainfall–runoff events. This provided us with the opportunity to study the hydrological responses of the system under contrasting conditions involving both dry and wet periods. On the other hand, there was no extreme rainfall episode with the return period larger than one year that would allow us to test the system under ponding conditions, and also no long-lasting wet period fed by persisting or recurrent rainfalls. This brings us back to the effect of the bimodal porosity of OPTI substrate. The bimodal character could result in slightly different retention capacity of the substrate leading to different behavior of the substrate under extreme and/or prolonged rainfalls. For a specific mineral soil substrate, Brunetti et al. (2016) reported that the bimodal porosity model was able to more accurately reproduce hydrographs in both dry and wet periods and to account for daily fluctuations of soil moisture than the unimodal model. However, bimodal character of green roof substrates is better expressed in dual permeability than bimodal porosity models (Vogel et al., 2000).

The surface temperature of our test beds is not measured directly, it is deduced indirectly from a single downward placed pyrgeometer. The pyrgeometer measurement is conducted about five meters apart from the test beds with the prevailing substrate underneath the sensor similar to TECH. For OPTI test bed, occasional inconsistencies between the observed soil temperature and the surface temperature calculated from pyrgeometer measurement were encountered. After some rainfall events, the soil temperature rose higher than the surface temperature. Such a phenomenon cannot be reproduced by the model, which thus predicts soil temperature lower than the observed one (highlighted points in Fig. 6). The discrepancy is most remarkable after moderate to major rainfall events. It is likely that the overall scatter of the OPTI-bed simulated-to-observed-temperature plot is related to this phenomenon. On the other hand, the temperature overestimation encountered for the TECH bed is probably related to the deficiency in the assessment of the soil thermal parameters.

In our modeling approach, we assumed that the plant transpiration dominates over the soil surface evaporation. It can be shown that the substrate surface becomes quickly dry after the cessation of rainfall leading to a sharp decrease of the surface hydraulic conductivity which in turn cuts off the soil surface from the soil moisture storage below. As can be seen in Fig. 3, the green roof system is designed so that a considerable amount of water stored in the system after a rainfall event is contained within the drainage board. This water has no direct hydraulic connection with the soil surface (it is separated by air from the soil layer above), still, it gradually disappears (the measured weight of the system implies so). Given the system structure, it can leave via evaporation and subsequent capillary condensation (Qin et al., 2016) or for the most part through the plant roots that connect the drainage board water storage with the atmosphere (i.e. via transpiration flux). The similarity between the simulated and measured rates of system drying during inter-rain intervals (Fig. 3) confirms that the plant transpiration of the studied system dominates the evapotranspiration process.

4. Conclusions

The soil water and thermal regimes of two green roof test beds were analyzed using a physically-based model. Comparison with observed outflow and temperature indicates that the green roof rainfall-runoff responses and temperature fluctuations can be successfully simulated by the presented modeling approach. The water-potential-gradient based root water uptake algorithm proved effective in capturing the water storage depletion between the rainfall events.

Hydrological functioning of the green roof can be similarly well captured with both Layered and Merged description of the soil profile. In both alternatives, the shape of retention curve, together with the applied bottom boundary condition, defines the water retention capacity of the system and thus is crucial for the appropriate evaluation of the roof hydraulic responses. However, when designing new green roofs, soil water retention data are rarely available, and even less measurements are available to calibrate physically-based models. Our experience suggests that a proper estimation of the difference between saturated and residual water content of soil substrate plays a key role, explaining the majority of discrepancies between measured and simulated outflow.

The difference between the two soil substrates tested in the present study (local TECH soil and commercial OPTI soil) is demonstrated by the contrasting ability of the soil layers to retain water. The Layered simulations reveal, that the TECH soil layer accounts for most of the retention capacity in the TECH test bed, while the OPTI layer has only minor effect in the OPTI test bed (as the respective drainage layer dominates). Moreover, the comparison of simulated water storage with the monitored weight of the OPTI test bed hints at a possibility of the dual-porosity effects on the effective retention capacity of the OPTI soil substrate.

Satisfactory model representation of the thermal conditions of the green roof test beds was achieved using independently evaluated thermal properties of the substrates and drainage board. This pleasing result is partly related to the fact that the roof system was very thin and the surface temperature was used as the upper boundary condition.

The effects of varying soil substrate thickness and vegetation type were evaluated on green roof water and thermal regimes. Increasing the substrate depth causes an increase of root water uptake (due to increasing retention capacity and longer travel times) and induces a significant reduction of the maximal temperature. The thinner soil profiles are also more sensitive to the type of plant species grown. The obtained results can be used to design green roofs under similar conditions.

Nomenclature.

Symbol	Name	Unit
General		
t	time	(s)
z	vertical coordinate	(m)
Water flow model		
θ	volumetric soil water content	($m^3\ m^{-3}$)
θ_r	residual water content	($m^3\ m^{-3}$)
θ_s	saturated water content	($m^3\ m^{-3}$)
h	soil water pressure head	(m)
K	soil hydraulic conductivity	($m\ s^{-1}$)
K_s	saturated hydraulic conductivity	($m\ s^{-1}$)
α_{VG}	empirical parameter determining the shape of water retention and unsaturated hydraulic conductivity functions	(cm^{-1})
n_{VG}	empirical parameter determining the shape of water retention and unsaturated hydraulic conductivity functions	(–)
Root water uptake model		
S	intensity of root water uptake	(s^{-1})
r_0	average active root radius	(m)
R	root length density	(m^{-2})
r_{soil}	soil hydraulic resistance	(s)
r_{root}	root radial resistance	(s)
H_{soil}	bulk-soil water potential	(m)
H_{rx}	root xylem water potential	(m)
H_{crit}	critical root xylem water potential	(m)
E_T	plant transpiration rate	($m\ s^{-1}$)
E_{Tp}	potential transpiration rate	($m\ s^{-1}$)
E_{Ta}	actual transpiration rate	($m\ s^{-1}$)

z_0	coordinate of the upper boundary of the root zone	(m)
z_R	coordinate of the lower boundary of the root zone	(m)
Heat transport model		
T	soil temperature	(K)
q	soil water flux	(m s^{-1})
ε_s	volumetric fraction of the soil mineral constituents	(–)
ε_o	volumetric fraction of the soil organic constituents	(–)
C	volumetric heat capacity of soil	(J $m^{-3} K^{-1}$)
C_w	volumetric heat capacity of water	(J $m^{-3} K^{-1}$)
C_s	heat capacity of solids	(kJ $kg^{-1} K^{-1}$)
λ	soil thermal conductivity	(W $m^{-1} K^{-1}$)
λ_{dry}	thermal conductivity for dry soil	(W $m^{-1} K^{-1}$)
λ_{sat}	thermal conductivity for saturated soil	(W $m^{-1} K^{-1}$)
κ	soil-type factor	(-)

Funding

Green roof systems and meteorological data were available through the courtesy of the University Centre for Energy Efficient Buildings, Czech Technical University in Prague. This study was supported by the Czech Science Foundation, project No. 17-21011S and by the Ministry of Education, Youth and Sports within National Sustainability Programme I, project number LO1605. Additional support was provided by the Grant Agency of the Czech Technical University in Prague, No. SGS18/171/OHK1/3T/11.

CRediT authorship contribution statement

Vojtech Skala: Formal analysis, Visualization, Writing - original draft. **Michal Dohnal:** Methodology, Writing - review & editing, Supervision. **Jana Votrubova:** Investigation, Writing - review & editing. **Tomas Vogel:** Conceptualization, Supervision. **Jaromir Dusek:** Software, Resources. **Jan Sacha:** Data curation, Resources. **Vladimira Jelinkova:** Data curation, Methodology.

References

Alexandri, E., Jones, P., 2007. Developing a one-dimensional heat and mass transfer algorithm for describing the effect of green roofs on the built environment: comparison with experimental results. Build. Environ. 42 (8), 2835–2849. https://doi.org/10.1016/j.buildenv.2006.07.004.

Bechmann, M., Schneider, C., Carminati, A., Vetterlein, D., Attinger, S., Hildebrandt, A., 2014. Effect of parameter choice in root water uptake models – the arrangement of root hydraulic properties within the root architecture affects dynamics and efficiency of root water uptake. Hydrol. Earth Syst. Sci. 18, 4189–4206. https://doi.org/10.5194/hess-18-4189-2014.

Brunetti, G., Šimůnek, J., Piro, P., 2016. A comprehensive analysis of the variably saturated hydraulic behavior of a green roof in a mediterranean climate. Vadose Zone J. 15. https://doi.org/10.2136/vzj2016.04.0032.

Côte, J., Konrad, J.M., 2005. A generalized thermal conductivity model for soils and construction materials. Can. Geotech. J. 42 (2), 443–485. https://doi.org/10.1139/t04-106.

D'Orazio, M., Di Perna, C., Di Giuseppe, E., 2012. Green roof yearly performance: a case study in a highly insulated building under temperate climate. Energy Build. 55, 439–451. https://doi.org/10.1016/j.enbuild.2012.09.009.

de Jong van Lier, Q., van Dam, J.C., Durigon, A., dos Santos, M.A., Metselaar, K., 2013. Modeling water potentials and flows in the soil-plant system comparing hydraulic resistances and transpiration reduction functions. Vadose Zone J. 12 (3). https://doi.org/10.2136/vzj2013.02.0039.

Djedjig, R., Ouldboukhitine, S.E., Belarbi, R., Bozonnet, E., 2012. Development and validation of a coupled heat and mass transfer model for green roofs. Int. Commun. Heat Mass Transf. 39 (6), 752–761. https://doi.org/10.1016/j.icheatmasstransfer.2012.03.024.

Doherty, J., Brebber, L., Whyte, P., 1994. Model-independent Parameter Estimation. User's Manual. Watermark Computing, Australia.

Durner, W., 1994. Hydraulic conductivity estimation for soils with heterogeneous pore structure. Water Resour. Res. 30 (2), 211–223. https://doi.org/10.1029/93WR02676.

Dvorak, B., Volder, A., 2010. Green roof vegetation for North American ecoregions: a literature review. Landsc. Urban Plan. 96 (4), 197–213. https://doi.org/10.1016/j.landurbplan.2010.04.009.

Feitosa, R.C., Wilkinson, S., 2016. Modelling green roof stormwater response for different soil depths. Landsc. Urban Plan. 153, 170–179. https://doi.org/10.1016/j.landurbplan.2016.05.007.

Guo, Y.P., Zhang, S.H., Liu, S.G., 2014. Runoff reduction capabilities and irrigation requirements of green roofs. Water Resour. Manage. 28 (5), 1363–1378. https://doi.org/10.1007/s11269-014-0555-9.

Hakimdavar, R., Culligan, P.J., Finazzi, M., Barontini, S., Ranzi, R., 2014. Scale dynamics of extensive green roofs: quantifying the effect of drainage area and rainfall characteristics on observed and modeled green roof hydrologic performance. Ecol. Eng. 73, 494–508. https://doi.org/10.1016/j.ecoleng.2014.09.080.

Hillel, D., 1998. Environmental Soil Physics. Academic Press, San Diego.

Hilten, R.N., Lawrence, T.M., Tollner, E.W., 2008. Modeling stormwater runoff from green roofs with HYDRUS-1D. J. Hydrol. 358 (3-4), 288–293. https://doi.org/10.1016/j.jhydrol.2008.06.010.

Jelinkova, V., Dohnal, M., Picek, T., 2015. A green roof segment for monitoring the hydrological and thermal behaviour of anthropogenic soil systems. Soil Water Res. 10 (4), 262–270. https://doi.org/10.17221/17/2015-SWR.

Jelinkova, V., Dohnal, M., Sacha, J., 2016. Thermal and water regime studied in a thin soil layer of green roof systems at early stage of pedogenesis. J. Soils Sediments 16 (11), 2568–2579. https://doi.org/10.1007/s11368-016-1457-7.

Ji, P., Sæbø, A., Stovin, V., Hanslin, H.H., 2018. Sedum root foraging in layered green roof substrates. Plant Soil 430, 263–276. https://doi.org/10.1007/s11104-018-3729-z.

Jim, C.Y., Peng Lilliana, L.L.H., 2012. Substrate moisture effect on water balance and thermal regime of a tropical extensive green roof. Ecol. Eng. 47, 9–23. https://doi.org/10.1016/j.ecoleng.2012.06.020.

Kodešová, R., Vlasáková, M., Fér, M., Teplá, D., Jakšík, O., Neuberger, P., Adamovský, R., 2013. Thermal properties of representative soils of the Czech Republic. Soil Water Res. 8, 141–150. https://doi.org/10.17221/33/2013-SWR.

Li, R., Peng, C., Chiang, P.C., Cai, Y.P., Wang, X., Yang, Z.F., 2019a. Mechanisms and applications of green infrastructure practices for stormwater control: a review. J. Hydrol. 568, 626–637. https://doi.org/10.1016/j.jhydrol.2018.10.074.

Li, S.X., Qin, H.P., Peng, Y.N., Soon, T.K., 2019b. Modelling the combined effects of runoff reduction and increase in evapotranspiration for green roofs with a storage layer. Ecol. Eng. 127, 302–311. https://doi.org/10.1016/j.ecoleng.2018.12.003.

Li, Y.L., Babcock, R.W., 2014. Green roofs against pollution and climate change. A review. Agron. Sustain. Dev. 34 (4), 695–705. https://doi.org/10.1007/s13593-014-0230-9.

Liu, T.C., Shyu, G.S., Fang, W.T., Liu, S.Y., Cheng, B.Y., 2012. Drought tolerance and thermal effect measurements for plants suitable for extensive green roof planting in humid subtropical climates. Energy Build. 47, 180–188. https://doi.org/10.1016/j.enbuild.2011.11.043.

Marquardt, D.W., 1963. An algorithm for least-squares estimation of nonlinear parameters. J. Soc. Ind. Appl. Math. 11 (2), 431–441. https://doi.org/10.1137/0111030.

Mentens, J., Raes, D., Hermy, M., 2006. Green roofs as a tool for solving the rainwater runoff problem in the urbanized 21st century? Landsc. Urban Plan. 77 (3), 217–226. https://doi.org/10.1016/j.landurbplan.2005.02.010.

Monteith, J.L., 1981. Evaporation and surface-temperature. Q. J. R. Meteorol. Soc. 107 (451), 1–27. https://doi.org/10.1256/smsqj.45101.

Monterusso, M.A., Rowe, D.B., Rugh, C.L., 2005. Establishment and persistence of Sedum spp. and native taxa for green roof applications. Hortscience 40 (2), 391–396. https://doi.org/10.21273/HORTSCI.40.2.391.

Nash, J.E., Sutcliffe, J.V., 1970. River flow forecasting through conceptual models part I – a discussion of principles. J. Hydrol. 10 (3), 282–290. https://doi.org/10.1016/0022-1694(70)90255-6.

Palla, A., Gnecco, I., Lanza, L.G., 2012. Compared performance of a conceptual and a mechanistic hydrologic models of a green roof. Hydrol. Process. 26 (1), 73–84. https://doi.org/10.1002/hyp.8112.

Palla, A., Sansalone, J.J., Gnecco, I., Lanza, L.G., 2011. Storm water infiltration in a monitored green roof for hydrologic restoration. Water Sci. Technol. 64 (3), 766–773. https://doi.org/10.2166/wst.2011.171.

Perez-Harguindeguy, N., Diaz, S., Garnier, E., Lavorel, S., Poorter, H., et al., 2013. New handbook for standardised measurement of plant functional traits worldwide. Aust. J. Bot. 61 (3), 167–234. https://doi.org/10.1071/BT12225.

Qin, H.-P., Peng, Y.-N., Tang, Q.-L., Yu, S.-L., 2016. A HYDRUS model for irrigation management of green roofs with a water storage layer. Ecol. Eng. 95, 399–408. https://doi.org/10.1016/j.ecoleng.2016.06.077.

Rieger, M., Litvin, P., 1999. Root system hydraulic conductivity in species with contrasting root anatomy. J. Exp. Bot. 50 (331), 201–209. https://doi.org/10.1093/jexbot/50.331.201.

Rosatto, H., Meyer, M., Laureda, D., Cazorla, L., Barrera, D., et al., 2013. Water retention efficiency of green roof systems in "extensive" and "intensive" type covers. Rev. Fac. Cienc. Agrar. 45 (1), 169–183.

Sailor, D.J., 2008. A green roof model for building energy simulation programs. Energy Build. 40 (8), 1466–1478. https://doi.org/10.1016/j.enbuild.2008.02.001.

Savi, T., Andri, S., Nardini, A., 2013. Impact of different green roof layering on plant water status and drought survival. Ecol. Eng. 57, 188–196. https://doi.org/10.1016/j.ecoleng.2013.04.048.

Schaap, M.G., Leij, F.J., van Genuchten, M.T., 2001. ROSETTA: a computer program for estimating soil hydraulic parameters with hierarchical pedotransfer functions. J. Hydrol. 251 (3–4), 163–176. https://doi.org/10.1016/S0022-1694(01)00466-8.

Skala, V., Dohnal, M., Votrubova, J., Jelinkova, V., 2019. The use of simple hydrological models to assess outflow of two green roofs systems. Soil Water Res. 14 (2), 94–103. https://doi.org/10.17221/138/2018-SWR.

Skerget, L., Tadeu, A., Brebbia, C.A., 2018. Transient numerical simulation of coupled heat and moisture flow through a green roof. Eng. Anal. Bound. Elem. 95, 53–68. https://doi.org/10.1016/j.enganabound.2018.06.018.

Starry, O., Lea-Cox, J.D., Kim, J., van Iersel, M.W., 2014. Photosynthesis and water use by two Sedum species in green roof substrate. Environ. Exp. Bot. 107, 105–112. https://doi.org/10.1016/j.envexpbot.2014.05.014.

Soulis, K.X., Valiantzas, J.D., Ntoulas, N., Kargas, G., Nektarios, P.A., 2017. Simulation of green roof runoff under different substrate depths and vegetation covers by coupling a simple conceptual and a physically based hydrological model. J. Environ. Manage. 200, 434–445. https://doi.org/10.1016/j.jenvman.2017.06.012.

Tabares-Velasco, P.C., Srebric, J., 2012. A heat transfer model for assessment of plant based roofing systems in summer conditions. Build. Environ. 49, 310–323. https://doi.org/10.1016/j.buildenv.2011.07.019.

van Genuchten, M.T., 1980. A closed-form equation for predicting the hydraulic conductivity of unsaturated soils. Soil Sci. Soc. Am. J. 44 (5), 892–898. https://doi.org/10.2136/sssaj1980.03615995004400050002x.

van Woert, N.D., Rowe, D.B., Andresen, J.A., Rugh, C.L., Fernandez, R.T., Xiao, L., 2005. Green roof stormwater retention: effects of roof surface, slope, and media depth. J. Environ. Qual. 34 (3), 1036–1044. https://doi.org/10.2134/jeq2004.0364.

Vesuviano, G., Stovin, V., 2013. A generic hydrological model for a green roof drainage layer. Water Sci. Technol. 68 (4), 769–775. https://doi.org/10.2166/wst.2013.294.

Vogel, T., Gerke, H.H., Zhang, R., van Genuchten, M. Th., 2000. Modeling flow and transport in a two-dimensional dual permeability system with spatially variable hydraulic properties. J. Hydrol. 238, 78–89.

Vogel, T., Brezina, J., Dohnal, M., Dusek, J., 2010b. Physical and numerical coupling in dual-continuum modeling of preferential flow. Vadose Zone J. 9 (2), 260–267. https://doi.org/10.2136/vzj2009.0091.

Vogel, T., Dohnal, M., Dusek, J., Votrubova, J., Tesar, M., 2013. Macroscopic modeling of plant water uptake in a forest stand involving root-mediated soil water redistribution. Vadose Zone J. 12 (1). https://doi.org/10.2136/vzj2012.0154.

Vogel, T., Dohnal, M., Votrubova, J., 2011. Modeling heat fluxes in macroporous soil under sparse young forest of temperate humid climate. J. Hydrol. 402 (3–4), 367–376. https://doi.org/10.1016/j.jhydrol.2011.03.030.

Vogel, T., Sanda, M., Dusek, J., Dohnal, M., Votrubova, J., 2010a. Using Oxygen-18 to study the role of preferential flow in the formation of hillslope runoff. Vadose Zone J. 9 (2), 252–259. https://doi.org/10.2136/vzj2009.0066.

Vogel, T., Votrubova, J., Dusek, J., Dohnal, M., 2016. Mesoscopic aspects of root water uptake modeling – hydraulic resistances and root geometry interpretations in plant transpiration analysis. Adv. Water Resour. 88, 86–96. https://doi.org/10.1016/j.advwatres.2015.12.006.

Wolf, D., Lundholm, J.T., 2008. Water uptake in green roof microcosms: effects of plant species and water availability. Ecol. Eng. 33 (2), 179–186. https://doi.org/10.1016/j.ecoleng.2008.02.008.

Yang, W.Y., Li, D., Sun, T., Ni, G.H., 2015. Saturation-excess and infiltration-excess runoff on green roofs. Ecol. Eng. 74, 327–336. https://doi.org/10.1016/j.ecoleng.2014.10.023.

Zwieniecki, M.A., Boersma, L., 1997. A technique to measure root tip hydraulic conductivity and root water potential simultaneously. J. Exp. Bot. 48 (307), 333–336. https://doi.org/10.1093/jxb/48.2.333.